JOURNAL OF GEOPHYSICAL RESEARCH, VOL. 88, NO. A8, PAGES 6171–6180, AUGUST 1, 1983

Terrestrial Versus Jovian VLF Chorus; A Comparative Study

U. S. INAN AND R. A. HELLIWELL

Space, Telecommunications and Radioscience Laboratory, Stanford University

W. S. KURTH

Department of Physics and Astronomy, University of Iowa

The relevant parameters of the magnetospheres of Jupiter and earth are studied from the point of view of wave-particle resonant interactions that are believed to be responsible for the generation of VLF chorus emissions observed on Voyager-1. Using existing models of the cold and energetic plasma distributions in the Jovian magnetosphere, expressions for the wave-particle interaction length (L_I) and the nonlinearity parameter (p) are derived. Values of these parameters are compared with those computed for the earth's magnetosphere. It is found that the typical interaction lengths are at least 2–5 times larger in the Jovian than in the terrestrial magnetosphere. Also, the wave intensity necessary to reach the threshold of nonlinearity in the Jovian magnetosphere was found to be up to 5–100 times lower. The Voyager 1 measurements show, however, that the inferred wave magnetic field intensities of the Jovian chorus are in the range of reported intensities for terrestrial chorus. This is attributed to fact that the fluxes of few keV resonant particles found in the Jovian magnetosphere were typically two orders of magnitude higher. In this case, it is predicted that the temporal growth rates of Jovian chorus bursts should be higher than for the earth. Growth rate measurements on Voyager 1 broadband wave data are used to confirm this hypothesis.

1. INTRODUCTION

Discrete chorus emissions in the earth's magnetosphere have been observed for decades. Appearing in the 100 Hz–30 kHz frequency range, these emissions usually consist of bands of overlapping variable frequency tones of 0.1–1.0 s duration and relatively narrow (<30 Hz) bandwidth [*Helliwell*, 1965]. Chorus emissions observed outside the plasmasphere usually appear to be spontaneous in origin [*Tsurutani and Smith*, 1974; *Burtis and Helliwell*, 1976] and often arise in a background of hiss. Inside the plasmasphere spontaneously generated emissions are not observed, and most discrete emissions are triggered by various input signals, such as whistlers, echoes of previous chorus, and VLF transmitter signals [*Helliwell*, 1965; *Helliwell and Katsufrakis*, 1974].

ELF/VLF chorus emissions are important for a number of reasons. Their narrowband and nonlinear character are evidence of a coherent natural plasma process that converts particle energy to electromagnetic radiation. Their relatively high intensities indicate that interactions of energetic particles with chorus emissions —and the resulting particle precipitation— may be an important loss process for the radiation belts. Understanding of the generation processes of these emissions may lead to the use of these emissions for the remote diagnostics of the radiation belt particle distributions. Observations of chorus emissions in the magnetospheres of Jupiter and Saturn makes the mechanism of chorus generation of wide general interest and have triggered the comparative analysis, which is the topic of this paper.

Paper number 3A0794.
0148-0227/83/003A-0794$05.00

Observations of plasma waves in general and VLF chorus in particular in the Jovian magnetosphere have been reported extensively [*Scarf et al.*, 1979; 1981 and references therein]. The Voyager 1 wideband wave receiver data has been particularly useful in identifying various kinds of plasma waves such as chorus, hiss, and lightning-generated whistlers. Implications of the detection of Jovian whistler mode chorus were discussed, and it was suggested that a significant portion of the observed Io torus aurora could be attributed to electrons precipitated as a result of resonant interactions with chorus waves [*Coroniti et al.*, 1980]. The energetic particle flux levels deduced from observations of chorus and hiss waves by the same authors were found to be in remarkable agreement with direct measurements [*Scudder et al.*, 1981]. The measured dispersion of lightning-generated whistlers and the cutoff frequencies of continuum radiation have been used to estimate the cold plasma density profile both along the field lines and as a function of radial distance from the planet [*Gurnett et al.*, 1981].

The purpose of this paper is to compare the characteristics of Jovian VLF chorus observed on Voyager 1 with the known parameters of terrestrial chorus. The results of this study will aid our understanding of the generation mechanisms of this naturally occurring coherent radiation phenomenon arising in planetary magnetospheres. To facilitate the analysis of the Jovian VLF data, Voyager 1 wideband receiver data are converted into analog form by the University of Iowa and sent to Stanford University for processing. The comparative study includes (1) comparison of observed parameters, i.e., normalized frequency (f/f_H), frequency-time slope (df/dt), wave intensity (B_w), and temporal growth rate (γ) and (2) comparison of parameter values relevant to a theoretical model of the coherent gyroresonant wave-particle interaction, i.e., the electron

density $N_e(z)$, electron gyrofrequency $\omega_H(z)$, the available interaction length L_I and the threshold field intensity required for trapping of the particles by the waves B_t.

2. Properties of Terrestrial Chorus

In this section we summarize some known characteristics of ELF/VLF chorus observed in the earth's magnetosphere [*Burtis and Helliwell*, 1969; 1975; 1976; *Tsurutani and Smith*, 1974]. Most of the published statistics were based on 600-700 different passes of the OGO 3 satellite.

1. Chorus was observed in the region $4 < L < 10$ during the period 0300–1500 LT.

2. Normalized mean chorus frequency (f/f_H) had a bimodal distribution with peaks near $f/f_H \approx 0.35$ and 0.55 and with a minimum at $f/f_H = 0.5$, where f_H is the equatorial gyrofrequency. Chorus frequency f tended to vary as L^{-3}.

3. The average slope df/dt varied roughly as L^{-2} with 50% of the cases having values in the 0.38 to 1.44 kHz/s range.

4. Peak chorus amplitudes ranged from 1 to 100 pT, with an average trend toward lower amplitudes at higher frequencies (lower L values) seen during long passes covering a wide L range.

5. Rising tones were more common (77%) than falling tones (16%) and other spectral shapes. The rate of occurrence of falling tones was much lower in the equatorial passes.

3. Properties of Jovian Chorus

We have examined the Voyager 1 wideband wave data to determine the occurrence and other properties of Jovian chorus emissions. The term 'chorus' as used in this study includes any discrete structured emissions with durations of 0.1–1.0 s, a definition that was also used to identify chorus in the earth's magnetosphere [*Burtis and Helliwell*, 1976]. The trajectory of the Voyager 1 spacecraft during its encounter with Jupiter on day 64 of 1979 is shown on a magnetic meridional plane plot in Figure 1. The regions of chorus observation are marked with thick lines. No discrete emission activity was observed outside those times.

An example of chorus activity observed by Voyager 1 is shown in Figure 2. The chorus emissions in this case are the discrete short duration rising tones in the 3 to 6 kHz range. The particular spectral shape of such emissions was found to be highly variable as in the case of terrestrial chorus. In this study, however, we consider only the average measurable properties of the chorus, specifically those that were listed in the previous section for chorus observed in the earth's magnetosphere.

To determine the normalized mean gyrofrequency at the time of chorus occurrence we have computed the gyrofrequency along the Voyager 1 trajectory. For this we have used the orbital parameters of the spacecraft in an internal field model of Jupiter's magnetic field that is corrected on the basis of Voyager 1 observations [*Connerney et al.*, 1982]. Figure 3 shows a plot of the electron gyrofrequency for the portion of the Voyager 1 trajectory covering L shells of 9.7–7.3. The two shaded areas indicate the occurrences of discrete chorus emissions; their lower and upper boundaries represent the lowest and highest frequencies of the chorus elements. This is only an average measure since there is some variation from one chorus element to the other.

Figure 3 shows that the center frequency has increased from the first observation of chorus ($L \simeq 8.88$) to the next, and that during the continuous observation around $L \simeq 8$ the chorus frequency showed a clear increase in time. Both observations indicate that chorus frequency follows the electron gyrofrequency f_H. In both cases the f/f_H ratio for chorus center frequency is very close to 0.4. The second observation also showed a second band of chorus at frequencies immediately above $f/f_H \simeq 0.5$. These features are remarkably similar to those of terrestrial chorus listed in item 2 of the previous section.

Another measurable property of the discrete emissions is the frequency-time slope, i.e., df/dt. In all identifiable chorus emission cases from Voyager 1 data, df/dt ranged from 0.8 to 1.2 kHz/s. Also, only rising tones were observed; no falling or hooklike emissions were seen. This result is similar to the OGO 3 observations of terrestrial chorus, in which the number of falling tones observed during equatorial passes was relatively low. Note from Figure 1 that the Voyager 1 trajectory was also not too far away from the magnetic equator.

4. Gyroresonant Wave-Particle Interactions

Cyclotron resonant interactions of energetic particles with whistler mode waves are believed to be responsible for the generation of discrete VLF emissions. In this section we derive general relationships for two important parameters that define the effectiveness of the phase-bunching process in these interactions, namely the interaction length L_I and the nonlinearity parameter ρ [*Helliwell*, 1967; *Nunn*, 1974; *Inan et al.*, 1978]. We then apply these separately to the terrestrial and Jovian cases in the following sections.

We consider the simple case of a circularly polarized monochromatic longitudinally propagating ($\mathbf{k} \| \mathbf{B}_0$) whistler mode wave for which the wave number k is given by

$$k \simeq \frac{\omega_P}{c}\left(\frac{\omega}{\omega_H - \omega}\right)^{1/2}, \qquad (1)$$

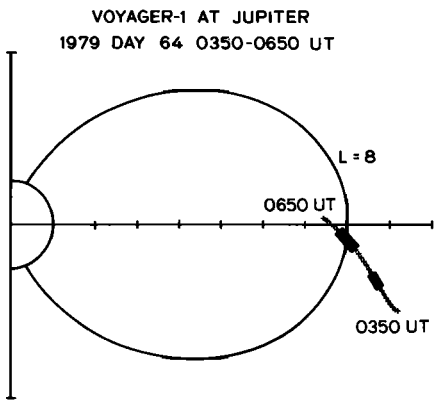

Fig. 1. The trajectory of Voyager-1 shown in a magnetic meridional plane on day 64 of 1979. Discrete chorus emissions were observed near 0457 UT and 0554-0642 UT.

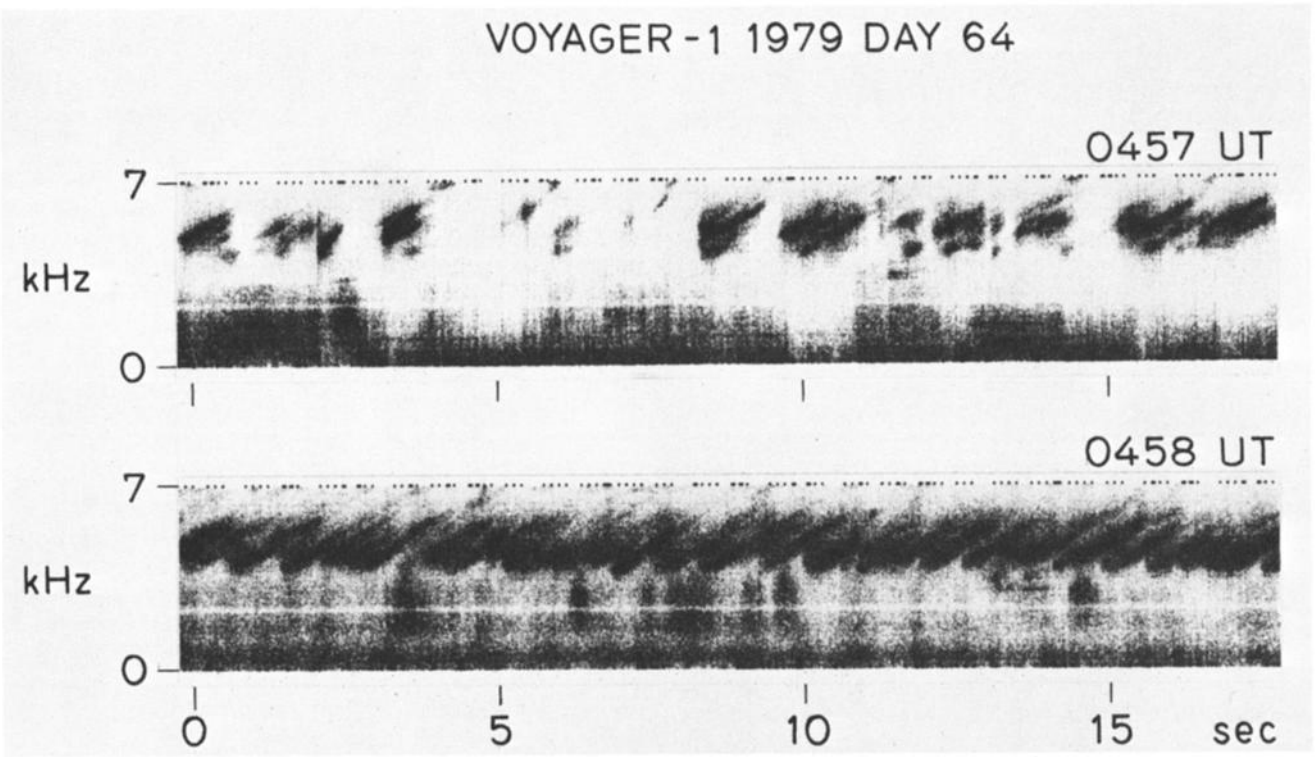

Figure 2. Examples of Jovian chorus emissions observed near 0457 UT. In this case the chorus emissions are in the 3 to 6-kHz range. Also seen is a background of hiss emissons in the 0 to 2-kHz range.

where c is the speed of light, ω_P is the electron plasma frequency, and ω and ω_H are the wave frequency and the electron gyrofrequency, respectively.

The relative motion of the gyrating particle and the circularly polarized wave during the resonant interaction is described by the rate of change of the angle ϕ between the particle's perpendicular velocity vector $\mathbf{v}_\perp$ and the wave magnetic field vector $-\mathbf{B}_w$. For particle pitch angles larger than a few degrees and for $B_w \ll B_0$, where B_0 is the static magnetic field this is given by

$$\frac{d\phi}{dt} \simeq \omega_H - \omega - kv_{||}, \tag{2}$$

where $v_{||}$ is the parallel velocity of the particle and where we have taken into account the fact that for the whistler mode wave with $\omega < \omega_H$, resonance can only occur with particles travelling in the direction opposite to $\mathbf{k}$. Significant energy exchange between the wave and the particle occurs when ϕ varies relatively slowly, i.e., $d\phi/dt \simeq 0$. The parallel velocity $v_{||}$ for which $d\phi/dt \simeq 0$ is denoted as the resonance velocity v_R.

During the resonant interaction the variation of the parallel velocity of the particle can be described as a superposition of the wave induced acceleration due to the $\mathbf{v}_\perp \times \mathbf{B}_w$ force and the adiabatic variation due to variation of B_0 (or ω_H) along the particle trajectory [*Dysthe*, 1971; *Inan et al.*, 1978]. Thus

$$\frac{dv_{||}}{dt} = \left(\frac{eB_w}{m}\right)v_\perp \sin\phi - \frac{v_\perp^2}{2\omega_H}\frac{d\omega_H}{dz}, \tag{3}$$

where e and m are the electronic charge and mass respectively where z is the distance along the field line with positive z being along the particle parallel velocity such that $v_{||} = dz/dt$. Differentiating (2) and using (3) we can obtain the generalized forced pendulum equation,

$$\frac{d^2\phi}{dt^2} + k\left(\frac{eB_w}{m}\right)v_\perp \sin\phi = \Pi(z) \tag{4}$$

where the inhomogeneity factor $\Pi(z)$ is given by

$$\Pi(z) = -\frac{v_{||}}{2N_e}(\omega_H - \omega)\frac{dN_e}{dz} + \left(\frac{3}{2} + \frac{\omega_H - \omega}{2\omega_H}\tan^2\alpha\right)v_{||}\frac{d\omega_H}{dz} \tag{5}$$

and N_e is the electron density. Since $\Pi(z)$ is dependent on the medium parameters $N_e(z)$ and $\omega_H(z)$, it is referred to as the inhomogeneity factor. It should be noted here that (4) and (5) or their equivalents have been derived by previous authors [*Dysthe*, 1971; *Inan et al.*, 1978; *Roux and Pellat*, 1978; *Bell and Inan*, 1981] but are repeated here for completeness.

The first of the two parameters of interest for describing the relative effectiveness of the phase-bunching process is the interaction length L_I, defined as the length of the region, centered around the magnetic equator, over which the phase ϕ would undergo a variation of π radians in the absence of the wave (B_w=0) [*Helliwell*, 1967; *Inan et al.*, 1978]. In other words,

$$\int_{-L_I/2}^{+L_I/2} (\omega_H - \omega - kv_{||}^u)\frac{dz}{v_{||}^u} \simeq \pi \tag{6}$$

where $v_{||}^u$ is the unperturbed particle parallel velocity that is obtained from (3) above with B_w=0. When the variations of the cold plasma parameters ($N_e(z)$ and $\omega_H(z)$) are known,

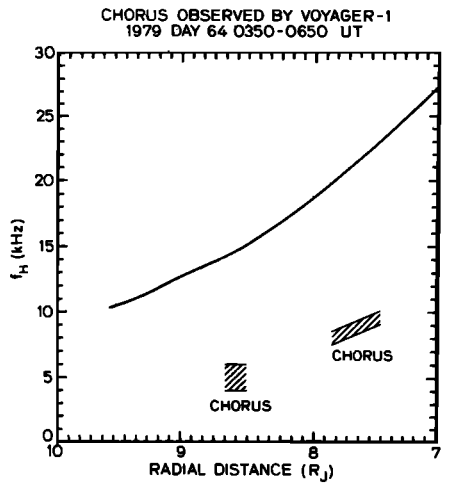

Fig. 3. Electron gyrofrequency along the Voyager-1 trajectory as obtained by using a corrected internal model of the Jovian magnetic field [*Connerney et al.*, 1981]. Also shown are the times of chorus observations. The upper and lower lines indicate the avarage upper and lower frequencies of individual chorus elements.

L_I can be obtained by twice integrating (4). Qualitatively, L_I represents the length of the region over which significant energy exchange between wave and particle can be expected to occur even for very small wave magnetic field intensities. The actual distance over which any given particle may stay in resonance with a given wave can actually be longer due to trapping of the particle by the wave [*Inan et al.*, 1978].

Whether or not there is significant trapping of particles by the wave depends on the relative magnitudes of the wave and inhomogeneity terms in (4). The ratio of these two terms provides a useful criterion for determining the transition from linearity (nearly unperturbed variation of ϕ) to nonlinearity (trapping leading to significantly perturbed ϕ) and is given by [*Inan et al.*, 1978]

$$\rho(z) = \frac{k\left(\frac{eB_w}{m}\right)v_\perp}{|\Pi(z)|} \simeq \frac{(\omega_H - \omega)\left(\frac{eB_w}{m}\right)\tan\alpha}{|\Pi(z)|} \qquad (7)$$

where α is the particle pitch angle and we have used $v_{||} \simeq v_R$ for the second equality. Note that $\rho(z)$ is a point measure, i.e.,it is the ratio of the maximum wave term to the inhomogeneity term at a given point z. However, when applied to the earth's magnetosphere it has been shown that ρ can be used to determine empirically whether or not nonlinear trapping effects need to be considered for the more general case when particle trapping is defined as the phase ϕ executing at least one complete oscillation [*Inan et al.*, 1978]. Thus it has been found that for $\rho > 1$ the wave forces are large enough to cause particle trapping and nonlinear effects, whereas for $\rho < 1$ the inhomogeneity term is dominant and the particle trajectory is approximately equal to the unperturbed (B_w=0) trajectory.

Since (7) cannot be evaluated at the magnetic equator ($z = 0$) where dN_e/dz and $d\omega_H/dz$ are both zero, for near equatorial interactions it has been shown that $\rho(z)$ evaluated at the edge of the unperturbed interaction region, i.e., -z=$L_I/2$, can be used as the nonlinearity threshold [*Inan et al.*, 1978]. In the following sections we evaluate and compare the values of the quantities L_I and ρ for wave-particle resonant interactions in the near equatorial regions of the magnetospheres of the earth and Jupiter.

5. EARTH'S MAGNETOSPHERE

The gyrofrequency $\omega_H(z)$ on closed field lines in the terrestrial magnetosphere varies approximately in accordance with a centered dipole model. In the close vicinity of the geomagnetic equator, the dipole variation is approximately parabolic [*Helliwell*, 1967]. This is useful for obtaining closed form expressions for the parameters of interest and is sufficient for the present analysis. Thus

$$\omega_H(z) = \omega_{H0}\left(1 + \frac{9z^2}{2L^2R_E^2}\right), \qquad (8)$$

where L is the L value, $R_E \simeq 6370$ km is the radius of the earth and ω_{H0} is the gyrofrequency at the equator (f_{H0} = 13.65 kHz at $L = 4$).

The cold plasma distribution along field lines in the earth's magnetosphere can be represented by either a diffusive equilibrium or a 'collisionless' model, depending on whether the region is inside or outside the plasmapause, respectively [*Angerami*, 1966; *Angerami and Carpenter*, 1966]. For a diffusive equilibrium model $dN_e/dz \simeq 0$ in the near vicinity of the equator. For a collisionless model the electron density N_e is approximately proportional to r^{-4}, where r is the radial distance. However, considerations of density recovery processes and recent experimental work [*Corcuff and Corcuff*, 1982] suggest that a variation as r^{-n}, with $n < 4$ may be more realistic.

Since most chorus was observed outside the plasmapause [*Burtis and Helliwell*, 1976], in this paper we assume a 'modified' collisionless model of the cold plasma for which N_e is proportional to r^{-3} everywhere. In this case, the variation along the field line of N_e and ω_H are approximately the same, since ω_H in a dipole model is also roughly proportional to r^{-3} for latitudes close to the magnetic equator [*Helliwell*, 1970]. Thus

$$N_e(z) \simeq N_{e0}\left(1 + \frac{9z^2}{2L^2R_E^2}\right), \qquad (9)$$

where N_{e0} is the equatorial cold plasma density.

Using (8), (9), and (2) we obtain from (5)

$$\Pi^E(z) = \frac{9\omega_H}{L^2R_E^2}\left[-\delta + \frac{3 + \delta\tan^2\alpha}{2}\right]v_{||}z \qquad (10)$$

where δ=$(\omega_H - \omega)/\omega_H$. In the above, the first term is due to dN_e/dz, whereas the second is due to $d\omega_H/dz$.

By twice integrating (4) with the assumption that $v_{||} \simeq v_{R0}$, $\omega_H \simeq \omega_{H0}$ and $\alpha \simeq \alpha_0$ and using (6) we obtain

$$L_I^E = \left[\frac{8v_RL^2R_E^2}{3f_H(3 + \delta\tan^2\alpha - 2\delta)}\right]^{1/3} \qquad (11)$$

where all quantities represent equatorial values so that we have dropped the subscript "0".

The nonlinearity parameter ρ can be evaluated by using (10) in (7). As mentioned above, $\rho(z)$ is computed at z=$L_I^E/2$ with L_I^E obtained from (11) Rather than com-

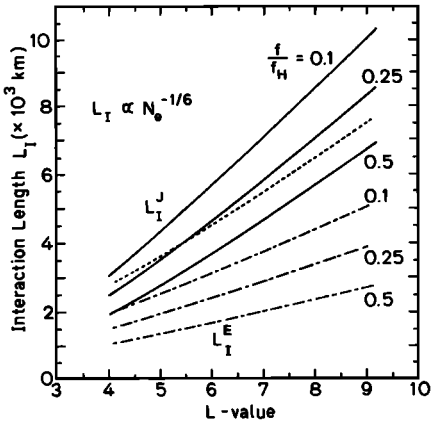

Fig. 4. Wave-Particle interaction length L_I versus L-value. The solid lines are the Jovian interaction lengths (L_I^J) for three different normalized frequencies $f/f_H = 0.1$, 0.25 and 0.5. The dashed lines are the same for the terrestrial interaction length (L_I^E). The dotted line shows L_I^J for f/f_H=0.5 computed by neglecting the $d\omega_H/dz$ term. The dependence of L_I on N_e is also shown.

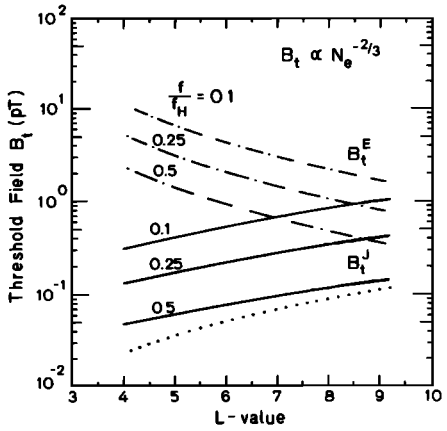

Fig. 5. Threshold field B_t versus L-value. The format is the same as in Figure 4.

puting ρ for an arbitrary value of B_w we have found it more revealing to calculate the wave magnetic field intensity B_w=B_t for which ρ=1. This then is referred to as the threshold field intensity, required for trapping and nonlinear effects to become significant [*Inan et al.*, 1978].

The dashed lines in Figures 4 and 5 show computed values of L_I^E and B_t^E, respectively, as a function of L value and for three different normalized frequencies f/f_H=1 − δ = 0.1, 0.25, and 0.5. The equatorial parallel resonant energy E_R^E is shown in Figure 6. The results given are for a pitch angle α=45° and for an equatorial cold plasma density N_{e0}=100 el/cc at L=4. Since N_e in (9) was assumed to vary everywhere as r^{-3} the equatorial density N_{e0} varies as L^{-3}. Since the density at L=4 can in fact vary between 10 and 800 el/cc [*Park et al.*, 1978], the N_e dependences of the parameters plotted are given on Figures 4, 5, and 6. In this case, L_I^E is proportional to $N_e^{-1/6}$ and B_t^E is proportional to $N_e^{-2/3}$. The resonant parallel energy E_R^E is proportional to N_e^{-1}.

6. JOVIAN MAGNETOSPHERE (NEAR IO TORUS)

The gyrofrequency $w_H(z)$ in the Jovian magnetosphere varies approximately as that of a dipole [*Acuna and Ness*, 1976]. For near equatorial regions this can be represented as a parabolic variation. In that case, the expression for $\omega_H(z)$ is identical to (8) with R_E replaced by the radius of Jupiter $R_J \simeq$ 71323 km. Also, the intensity of the static field is somewhat different so that $f_{H0} \simeq$ 22.4 kHz at $L \simeq$ 8. Here again, we neglect the effects of field line distortion for this first order analysis.

The equatorial electron density in the vicinity of the Io torus over L shells of 6–10 in the Jovian magnetosphere was found to vary as $r^{-7.4}$ [*Bagenal et al.*, 1980; *Bagenal and Sullivan*, 1981; *Gurnett et al.*, 1981; *Birmingham et al.*, 1981]. The variation of the cold plasma density N_e along the field line is assumed to be given by

$$N_e(z) = N_{e0} \exp\left[-\left(\frac{z}{H}\right)^2\right], \qquad (12)$$

where the scale height $H \simeq R_J$ at $L \simeq 8$ where chorus was observed. However, there is enough uncertainty in the modeling so that the scale height could be as high as $2R_J$ [*Gurnett et al.*, 1981]. In this paper we use $H \simeq R_J$. For the absolute level of the plasma density we use $N_{e0} \simeq$ 230 el/cc at $L \simeq 8$ based upon measurments by Voyager 1 [*Bagenal et al.*, 1980].

With $\omega_H(z)$ and $N_e(z)$ determined as described above, we use (8), (12), and (2) to obtain from (5)

$$\Pi^J(z) = \left[\frac{\delta\omega_H}{H^2} + \frac{9\omega_H}{2L^2R_J^2}(3 + \delta\tan^2\alpha)\right]v_{\|}z \qquad (13)$$

where the second term is due to $d\omega_H/dz$ and thus is similar to the second term in (10). The first term is due to dN_e/dz and is different because of the difference between (9) and (12). It should be noted that while the first term in (10) has little effect in comparison with the second term, in (13) the first term is dominant especially for higher L values. Thus the inhomogeneity factor in the Jovian magnetopshere is mainly controlled by the variation of $N_e(z)$ rather than $\omega_H(z)$, as in the terrestrial magnetosphere.

By the same procedure used in obtaining (11) we find from (4), (6), and (13) that

$$L_I^J = \left[\frac{48v_RL^2R_J^2H^2}{2f_H\delta L^2R_J^2 + 9H^2f_H(3 + \delta\tan^2\alpha)}\right]^{1/3} \qquad (14)$$

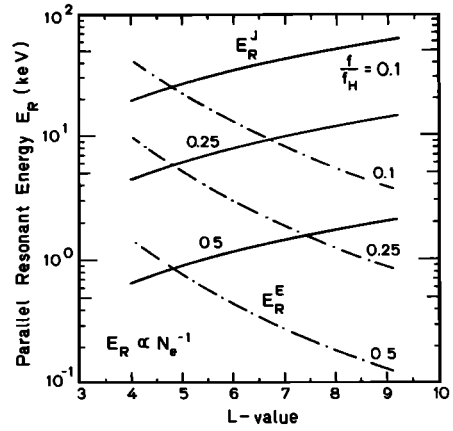

Fig. 6. Parallel resonant energy E_R versus L-value. The format is the same as in Figure 4.

TABLE I. Comparison of Parameter Values

	L	N_e (el/cc)	f_H (kHz)	f (kHz)	E_R (keV)	L_I (km)	B_t (pT)
Earth	4	30	13.65	6.8	4.9	1280	5.3
Jupiter	8	230	22.4	11.2	1.7	5642	0.12

where as in (11) all quantities represent equatorial values.

As in the terrestrial case the threshold field intensity B_t^J for which $\rho(L_I^J/2)=1$ can be computed by using (14) and (13) in (7). The solid lines in Figures 4 and 5 show computed values of L_I^J and B_t^J, respectively, as a function of L value and for three different normalized frequencies. The equatorial parallel resonant energy E_R^J is given in Figure 6. The results given are for a particle pitch angle $\alpha_0 = 45°$ and an equatorial cold plasma density $N_{e0} = 230$ el/cc at L=8. The N_e dependence of the Jovian parameters plotted in Figures 4, 5, and 6 are identical to those for the terrestrial parameters.

Also shown as a dotted line in Figures 4 and 5 are L_I^J and B_t^J for $f/f_H = 0.5$, computed using only the first or dNe/dz term in (13). These results show that these parameter values are for the most part determined by the variation of the electron density. As expected, the effect of $d\omega_H/dz$ is more significant at lower L values as expected, but even at $L = 4$ the error that results from neglecting the second term in (13) is less than 10%. This result is interesting because it contrasts with the terrestrial case, where L_I and B_t are mainly determined by $d\omega_H/dz$.

Another difference between the two magnetospheres can be seen by comparing the parameters in Figure 5, which show that B_t^E decreases with increasing L whereas B_t^J is higher on higher L shells. This is due to the fact that since the scale height H is assumed to be the same on all L shells considered, the inhomogeneity factor $\Pi^J(z)$ does not vary rapidly with L.

Note that neglecting the second term in (13) amounts to dropping the second term in the denominator of (14). It can then be seen that the interaction length L_I^J is roughly proportional to $H^{2/3}$. The threshold field B_t^J on the other hand is proportional to H^2. Since the results given in Figures 4 and 5 are given for $H=R_J$, these dependences can be used to estimate the parameter values for other H. For example, for $H=2R_J$, the L_I^J values would be smaller by a factor of 1.6, whereas B_t^J would be higher by a factor of 4. A simpler expression for the interaction length L_I^J for the case in which the second term in (15) is neglected can be written as

$$L_I^J = \left[\frac{24 v_R H^2}{f_H - f}\right]^{1/3}, \qquad (16)$$

7. Comparison of Parameter Values

Using the results given in Figures 4-6, we can quantitatively compare parameter values relevant to the gyroresonant wave-particle interaction for the Jovian and terrestial magnetospheres. In general we see that the interaction length L_I is 2–5 times larger in the Jovian magnetosphere whereas the threshold field B_t^J can be up to 5–100 times lower depending on L value.

Instead of comparing parameters on the same L shells, it is more interesting to compare a typical terrestrial case outside the plasmapause with $L \simeq 8$ in the Jovian magnetosphere where chorus was observed on Voyager 1. For the earth's magnetosphere, we have taken $L \simeq 4$, and $N_{e0} =$ 30 el/cc. The parameter values for these two cases are listed in Table 1. It is seen that while f_H, f and the resonant particle energy E_R are quite similar, the interaction length L_I for the Jovian case is a factor of $\simeq$4.4 higher. The difference in the threshold field intensities B_t is even larger with B_t a factor of $\simeq$45 higher for the terrestrial case.

In light of this result, one might expect chorus intensities to be a factor of roughly 10-100 times lower at Jupiter than at earth. In other words, if the commonly observed saturation of temporal growth of spontaneous and triggered emissions [*Helliwell and Katsufrakis*, 1974] is related to the field intensity at which nonlinear effects begin, then the higher threshold fields B_t^E would imply that the observed chorus intensities would also be higher for terrestrial chorus. This is a reasonable expectation since all that is required is that the saturation field be 'related' to B_t, allowing for the possibility that it could indeed be higher than B_t itself. The relation between the threshold field and the observed saturation levels is assumed to be the same in both magnetospheres, however.

Intensities of Jovian chorus emissions observed on Voyager 1 in the vicinity of $L \simeq 8$ have been reported to be roughly 0.2 mV/m, corresponding to $\simeq$ 10 pT for assumed parallel propagation and the observed cold plasma parameters [*Coroniti et al.*, 1980]. In view of the above, this observation would be equivalent to observation of chorus intensities of 450 pT in the earth's magnetosphere. Such levels would be significantly higher than even the maximum intensities reported [*Burtis and Helliwell*, 1976]. It was noted above that if we assumed the scale height $H \simeq 2R_J$, the B_t^J values would be a factor of 4 lower. Even if this was the case, the observed 10 pT intensities would correspond to 115 pT in the earth's magnetosphere still at least well on the higher side of the intensities reported for terrestrial chorus.

This apparent anomaly may be due to the different levels of energetic particle fluxes in the terrestrial and Jovian magnetospheres. In the earth's magnetosphere outside the plasmapause differential energy spectra of electrons with 1 to 10-keV energy range from $\Phi^E \simeq 10^5$ to 10^8 el/cm^2-s-sr-keV [*Schield and Frank*, 1970; *Lyons and Williams*, 1975]. However, during the Voyager-1 traverse of the Io torus the measured fluxes of few keV particles were $\Phi^J \simeq 10^{10}$ el/cm^2-s-sr-keV

[*Scudder et al.*, 1981]. This difference could explain the comparatively higher chorus intensities that are reported for the Jovian magnetosphere.

While both triggered and spontaneous discrete VLF emissions clearly show a saturation effect [*Burtis and Helliwell*, 1976; *Helliwell and Katsufrakis*, 1974], the physics of the saturation mechanism is still not well understood [*Nunn*, 1974; *Matsumoto*, 1978]. Thus, the observations in the magnetosphere of Jupiter may be the first evidence that the saturation level is higher for higher fluxes of energetic particles. On the other hand, if the saturation levels are not related to the trapped particle flux, then the above discussion may serve as a means of estimating the scale height H. In other words, one could argue that if the relation between saturation level and B_t is indeed the same in both magnetospheres, observation of 10 pT field intensities for Jovian chorus may imply that $B_t^J \simeq B_t^E$. For this to be true, the scale height for the electron density variation should be in the range of $\simeq 4 - -6R_J$. In any case, it is clear that the Jovian chorus observed by Voyager 1 presents us with a unique opportunity to improve our understanding of the generation mechanisms of discrete VLF emissions.

8. TEMPORAL GROWTH RATE

From the preceding discussion, it is evident that a measurable parameter is needed to clarify our understanding of the wave-particle interactions that are believed to be responsible for the generation of chorus emissions. One such parameter is the temporal growth rate (γ). In general, the growth rate during the wave-particle interaction is expected to be proportional to the available particle fluxes and to the anisotropy of the energetic particle distribution function [*Kennel and Petschek*, 1966; *Helliwell*, 1967; *Helliwell and Inan*, 1982]. In the following we shall assume that the anisotropy factors in the Jovian and terrestrial energetic particle distributions are on the average the same so that we can compare the expected temporal growth rates.

From the feedback model of gyroresonant wave-growth and triggering in the magnetosphere [*Helliwell and Inan*, 1982] the temporal growth rate γ is given by

$$\gamma = \frac{v_{\parallel}}{L_I}(G-1) \tag{17}$$

where G is the feedback loop gain, a quantity proportional to (among other things such as the anisotropy) the trapped resonant particle flux Φ. Assuming $(G-1) \simeq G$ the ratio of the Jovian to terrestrial temporal growth rates is

$$\frac{\gamma^J}{\gamma^E} \simeq \frac{v_{\parallel}^J L_I^E \Phi^J}{v_{\parallel}^E L_I^J \Phi^E} \tag{18}$$

The growth rate ratios normalized to $\Phi^E = \Phi^J$, are plotted in Figure 7 versus L value and for f/f_H=0.1, 0.25, and 0.5. The other parameter values for Figure 7 were taken to be the same as in Figures 4-9. Without the factor of at least 100 difference in the trapped radiation flux levels, the temporal growth rates for the terrestrial and Jovian chorus are within a factor of 2 of each other. Allowing for the difference in flux levels significantly higher growth rates should be expected for the Jovian magnetosphere.

To compare a typical Terrestrial case with the Voyager

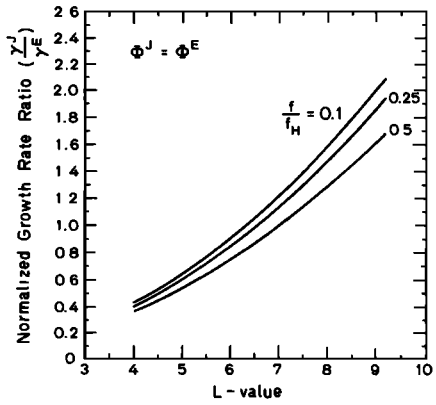

Fig. 7. Normalized growth rate ratio γ^J/γ^E versus L-value for $\Phi^J = \Phi^E$.

1 examples of chorus (rather than comparing parameters on the basis of the same L value) we use the parameters given in Table 1. Then for $\Phi^J = 10^{10}$ and $\Phi^E = 10^8$ el/cm^2-s-sr-keV we obtain

$$\frac{\gamma^J}{\gamma^E} \simeq 13$$

assuming as mentioned above that the other factors (e.g.,anisotropy) on which the growth rate depends are the same for both cases.

In order to check the predicted higher growth rates for the Jovian chorus, we have processed the Voyager 1 wideband data for amplitude and spectral information. Figure 8 shows two isolated chorus bursts observed at $L \simeq 8.8$ at the outer edge of the Io torus. The top panel shows spectra in the 0 to 7-kHz range. The second panel (from top) shows the amplitude of the chorus element indicated by a frequency-tracking filter. The third panel shows the center frequency of the tracking filter (a 1-kHz bandwidth). The standby frequency for the tracking filter was chosen to be 4.6 kHz. Since AGC information from the receiver is not available, we used other features of the data that could be expected to remain constant on the time scale considered. The bottom panel shows the intensity in a 300-Hz bandwidth centered at 500 Hz where a relatively steady hiss emission was observed (see top panel for spectrum). Thus the bottom panel gives a rough indication of the AGC voltage level of the receiver. Since this remains constant during the course of the first chorus burst, an estimate of the temporal growth rate can be made. From the second panel we estimate that the growth rate is $\sim$800 dB/s for the first emission and even higher for the second one. The fact that the growth takes place in $\sim$30 ms increases our confidence in this measurement since the response time constant of the AGC system is $\sim$250 ms.

The fact that the growth takes place in such a short time is also indicative of the fact that the observed signal level increase is due to the temporal growth of the wave rather than a spatial effect having to do with the spacecraft moving into an existing wave packet. This is so because the wavelength of the whistler mode waves is of the order of 1–2 km and the satellite speed is also of the order of few km/s. Thus for the observed signal increase to be due to a spatial effect, the wave packet must be confined to regions in space of size comparable to a wavelength. It is for this reason that the observed growth of the signal is

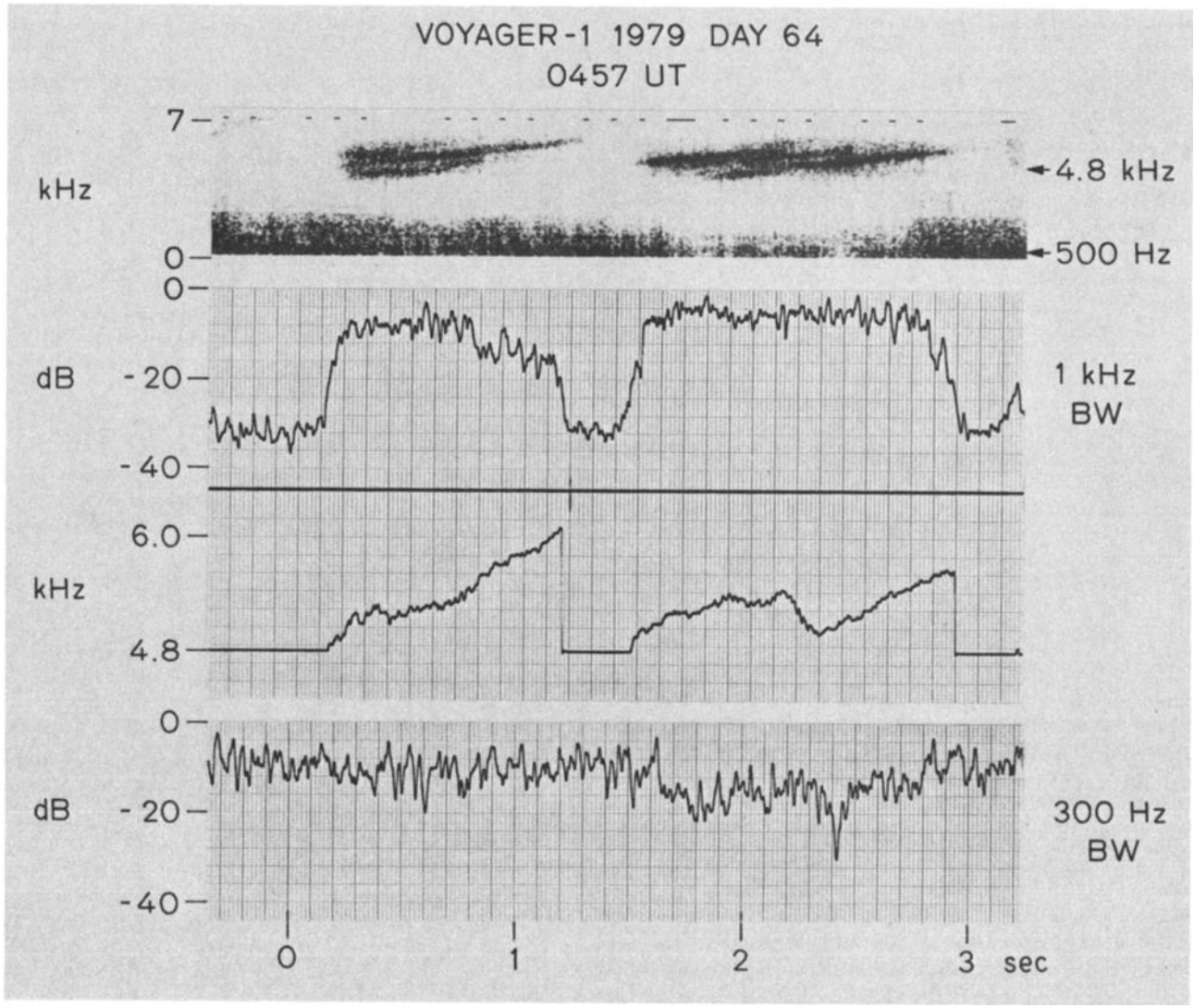

Figure 8. Top panel shows two multielement Jovian chorus bursts. The second panel shows the amplitude of the chorus element indicated by a frequency tracking filter. The third panel shows the center frequency of the tracking filter (1 kHz bandwidth). The standby frequency for the tracking filter was chosen to be 4.8 kHz. The bottom panel shows the intensity in a 300 Hz bandwidth centered at 500 Hz where a relatively steady hiss emission is seen (top panel).

believed to be due to the temporal wave growth at the time of the generation of the chorus emission. The generation region may indeed not be at the satellite location, since in the absence of significant dispersion (frequency range of individual elements are small) the signal would retain its temporal shape during its propagation from the source to the receiver.

While more accurate growth rate measurements are necessary, the one case shown in Figure 8 indicates that the growth rates for Jovian chorus are at least on the higher side of the range of growth rates measured for terrestrial chorus (200–2000 dB/s). In fact, growth rates higher than 750 dB/s were very rarely observed in the earth's magnetosphere [*Burtis and Helliwell,* 1976]. Thus our expectations on the basis of the theory above are at least not inconsistent with the data, considering the large uncertainties in measured growth rates and particle fluxes.

9. Summary and Conclusions

In summary, we can list the properties of Jovian chorus as measured on Voyager-1 wideband data as follows:

1. Chorus was observed in the region $7.5 < L < 9$, i.e., in the outer part of the Io torus. No chorus was observed well inside the torus ($L \simeq 6$), where lightning generated whistlers were observed [*Gurnett et al.,* 1981]

2. The mean chorus frequency tended to follow f_H, with peaks near $f/f_H \simeq 0.4$ and 0.6 and a minimum at 0.5

3. The slope df/dt was in the 0.8-1.2 kHz/s range

4. The measured field intensity of chorus was about 0.26 mV/m, corresponding to $\simeq$ 10 pT for parallel propagation [*Coroniti et al.,* 1980]

5. Only rising tone emissions were observed

6. Measured growth rates exceeded 750 dB/sec. More accurate measurements of growth rate are needed

Theoretical calculations of the wave-particle interaction length and the threshold field intensity for nonlinear effects to become significant showed that

1. The interaction length in the Jovian magnetosphere is typically 2-5 times larger than in the terrestrial case.

2. The threshold field intensity in the Jovian magnetosphere is 5-100 times lower than that in the earth's magnetopshere.

3. For the inferred wave magnetic field intensities (10 pT) in the Jovian magnetosphere, the nonlinearity parameter $\rho \gg 1$, indicating that the interaction and thus the particle trajectories are highly nonlinear. In such a case large pitch angle scattering of individual particles can be expected [*Inan et al.,* 1978; *Bell and Inan,* 1981], and in general a test particle simulation approach is needed to analyze the energy exchange between the waves and particles. For the same reason, linear formulations of the wave-particle interaction [*Kennel and Petschek,* 1966] would not be applicable.

4. Temporal growth rates are expected to be higher in the Jovian than in the terrestrial magnetosphere.

As noted in section 7, our results for B_t^J and L_I^J depend on the scale height of the electron density variation along the field lines, namely H. For the parameters given in Figures 4 and 5 we have used $H \simeq R_J$. However, the scale height can be expected to be as high as $2\text{-}2.5R_J$, depending on the field line of propagation [*Gurnett et al.,* 1981]. Since B_t^J is proportional to H^2, even $H \simeq 2.5R_J$ would give B_t values that can be 1-16 times larger at Jupiter than at earth. For the parameters of Table 1, $B_t^J \simeq B_t^E$ requires $H \simeq 6R_J$. Thus our results imply either that the saturation levels for spontaneous emissions are proportional to trapped particle fluxes or that the scale height H for the electron density variation along the field lines is higher than previously estimated.

We note from (16) that the dependence of L_I^J on H is not nearly as critical as that of B_t^J. Because of this and the at least two orders of magnitude difference between Φ^J and Φ^E, it is evident from (18) that the ratio of the Jovian and terrestrial growth rates would also not depend critically on the value of H. Thus, temporal growth rate may indeed constitute an important measurable parameter that can be used to check our understanding of chorus phenomena observed in the magnetosphere of Jupiter as well as possibly other planets.

In conclusion, we can say that while there are many similarities between terrestrial and Jovian chorus, there seem to be important differences in the theoretical parameters that are relevant to the mechanisms assumed to be responsible for emission generation. Study of these differences and the application of the results to other planetary phenomena (e.g., Saturnian chorus) should help to advance our understanding of this coherent radiation phenomenon. Controlled wave-injection experiments in the earth's magnetosphere, using ground or satellite based VLF transmitters could also provide much needed understanding of the generation mechanism of this coherent radiation phenomena that seems to arise in planetary magnetospheres.

Acknowledgments. We thank our colleagues in the VLF group at Stanford for their helpful comments, K. Faes for typing the manuscript, and A. Leach for doing the figures. We also thank D. Hinson for running the Jovian magnetic field model used for Figure 3. The research at Stanford University was supported by the National Aeronautics and Space Administration under contract NAGW-164. We also thank F. L. Scarf and D. A. Gurnett for making the Voyager 1 wideband data available. The work at University of Iowa was supported by NASA under grant NAGW-337 and contract No. 954013 with the Jet Propulsion Laboratory.

The Editor thanks F. Scarf and another referee for their assistance in evaluating this paper.

REFERENCES

Acuna, M. H., and N. F. Ness, Results from the GSFC fluxgate magnetometer on Pioneer 11, in *Jupiter,* edited by T. Gehrels, pp. 830-847, University of Arizona Press, Tucson, 1976.

Angerami, J. J., A whistler study of the distribution of thermal electrons in the magnetosphere, *Tech. Rep. 3412-7,* Radiosci. Lab., Stanford Electron. Lab., Stanford Univ., Stanford, Calif., 1966.

Angerami, J. J., and D. L. Carpenter, Whistler studies of the plasmapause in the magnetosphere, 2, Equatorial density and total tube electron content near the knee in magnetospheric ionization, *J. Geophys. Res., 71,* 711, 1966.

Bagenal, F., and J. D. Sullivan, Direct plasma measurement in the Io torus and inner magnetosphere of Jupiter, *J. Geophys. Res., 86,* 8447, 1981.

Bagenal, F., J. D. Sullivan, and G. L. Siscoe, Spatial distribution of plasma in the Io torus, *Geophys. Res. Lett., 7,* 41, 1980.

Bell, T. F., and U. S. Inan, Transient nonlinear pitch angle scattering of energetic electrons by coherent VLF wave packets in the magnetosphere, *J. Geophys. Res., 86,* 9047, 1981.

Birmingham, T. J., J. K. Alexander, M. D. Desch, R. F. Hubbard, and B. M. Petersen, Observations of electron gyroharmonic waves and the structure of the Io Torus, *J. Geophys. Res., 86(A10),* 8497, 1981.

Burtis, W. J., and R. A. Helliwell, Banded chorus: A new type of VLF radiation observed in the magnetosphere by OGO-1 and OGO-3, *J. Geophys. Res., 74,* 3002, 1969.

Burtis, W. J., and R. A. Helliwell, Magnetospheric chorus: Amplitude and growth rate, *J. Geophys. Res., 80,* 3265, 1975.

Burtis, W. J., and R. A. Helliwell, Magnetospheric chorus: Occurrence patterns and normalized frequency, *Planet. Space Sci., 24,* 1007, 1976.

Connerney, J. E. P., M. H. Acuna, and N. F. Ness, Voyager 1 assessment of Jupiter's planetary magnetic field, *J. Geophys. Res., 86,* 3623, 1982.

Corcuff, Y., and P. Corcuff, Structure et dynamique de la plasmapause - plasmasphere les 6 et 14 juillet 1977: etude a l'aide des donnees de sifflements recus au sol et de donnees des satellites ISIS et GEOS-1, *Ann. Geophys., t.38, fasc. 1,* 1, 1982.

Coroniti, F. V., F. L. Scarf, C. F. Kennel, W. S. Kurth, and D. A. Gurnett, Detection of Jovian whistler mode chorus: Implications for the Io torus aurora, *Geophys. Res. Lett., 7,* 45, 1980.

Dysthe, K. B., Some studies of triggered whistler emissions, *J. Geophys. Res., 76,* 6915, 1971.

Gurnett, D. A., F. L. Scarf, W. S. Kurth, R. R. Shaw, and R. L. Poynter, Determination of Jupiter's electron density profile from plasma wave observations, *J. Geophys. Res., 86,* 8199, 1981.

Helliwell, R. A., *Whistlers and Related Ionospheric Phenomena,* Stanford University Press, Stanford, Calif., 1965.

Helliwell, R. A., A theory of discrete VLF emissions from the magnetosphere, *J. Geophys. Res., 72,* 4773, 1967.

Helliwell, R. A., Intensity of discrete VLF emissions, in *Particles*

and Fields in the Magnetosphere, edited by B. M. McCormac, p. 292, Dordrecht, D. Reidel, 1970.

Helliwell, R. A., and U. S. Inan, VLF wave growth and discrete emission triggering in the magnetosphere: A feedback model, *J. Geophys. Res., 87,* 3537, 1982.

Helliwell, R. A., and J. P. Katsufrakis, VLF wave injection into the magnetosphere from Siple Station, Antarctica, *J. Geophys. Res., 79,* 2511, 1974.

Inan, U. S., T. F. Bell, and R. A. Helliwell, Nonlinear pitch angle scattering of energetic electrons by coherent VLF waves in the magnetosphere, *J. Geophys. Res., 83,* 3235, 1978.

Kennel, C. F., and H. E. Petschek, Limit on stably trapped particle fluxes, *J. Geophys. Res., 71,* 1, 1966.

Lyons, L. R., and D. J. Williams, The quiet time structure of energetic (35-560 keV) radiation belt electrons, *J. Geophys. Res., 80,* 943, 1975.

Matsumoto, H., Nonlinear whistler mode interaction and triggered emissions in the magnetosphere: A review. *Wave Instabilities in Space Plasma,* published by D. Reidel, 1978.

Nunn, D., A self-consistent theory of triggered VLF emissions, *Planet. Space Sci., 22,* 349, 1974.

Park, C. G., and D. L. Carpenter, and D. B. Wiggin, Electron density in the plasmasphere: Whistler data on solar cycle, annual, and diurnal variations, *J. Geophys. Res., 83,* 3137, 1978.

Roux, A., and R. Pellat, A theory of triggered emissions, *J. Geophys. Res., 83,* 1433, 1978.

Scarf, F. L., D. A. Gurnett, and W. S. Kurth, Jupiter plasma wave observations: An initial Voyager 1 overview, *Science, 204,* 991, 1979.

Scarf, F. L., D. A. Gurnett, and W. S. Kurth, Measurements of plasma wave spectra in Jupiter's magnetosphere, *J. Geophys. Res., 86,* 8181, 1981.

Schield, M. A., and L. A. Frank, Electron observations between the inner edge of the plasma sheet and the plasmasphere, *J. Geophys. Res., 75,* 5401, 1970.

Scudder, J. D., and E. C. Sittler, Jr., and H. S. Bridge, A survey of the plasma electron environment of Jupiter: A view from Voyager, *J. Geophys. Res., 86,* 8157, 1981.

Tsurutani, B. T., and E. J. Smith, Postmidnight chorus: A substorm phenomenon, *J. Geophys. Res., 79,* 118, 1974.

U. S. Inan and R. A. Helliwell, Space, Telecommunications, and Radioscience Laboratory, Stanford University, Stanford, CA 94305.

W. S. Kurth, Department of Physics and Astronomy, University of Iowa, Iowa City, IA 52242.

(Received March 31, 1983;
revised May 9, 1983;
accepted May 16, 1983.)